On thermionic emission and the use of vacuum tubes in the advanced physics laboratory

Paul J. Angiolillo

Department of Physics, Saint Joseph's University, 5600 City Avenue, Philadelphia, Pennsylvania 19131

Two methods are outlined for measuring the charge-to-mass ratio e/m_e of the electron using thermionic emission as exploited in vacuum tube technology. One method employs the notion of the space charge in the vacuum tube diode as described by the Child–Langmuir equation; the other method uses the electron trajectories in vacuum tube pentodes with cylindrical electrodes under conditions of orthogonally related electric and magnetic fields (the Hull magnetron method). The vacuum diode method gave $e/m_e = 1.782 \pm 0.166 \times 10^{+11}$ C/kg (averaged over the vacuum diodes studied), and the Hull magnetron method gave $e/m_e = 1.779 \pm 0.208 \times 10^{+11}$ C/kg (averaged over both pentodes and the anode voltages studied). These methods afford opportunities for students to determine the e/m_e ratio without using the Bainbridge tube method and to become familiar with phenomena not normally covered in a typical experimental methods curriculum. © *2009 American Association of Physics Teachers.*
[DOI: 10.1119/1.3212463]

I. INTRODUCTION

No course in experimental modern physics is complete without evaluating the charge-to-mass ratio of the electron. This experiment is typically done using the Bainbridge apparatus;[1–3] this apparatus generates values of the charge-to-mass ratio that are $\leq 10\%$ in accuracy.

The release of electrons from heated metals has a long and interesting history, and although there are numerous anecdotal accounts of related electrical phenomena, the first systematic studies were performed in the early 1880s. The most celebrated of these were the experiments of Thomas Edison as a spin-off of his attempts to develop a long-lasting incandescent light bulb. The vacuum diode was inadvertently invented in 1883 by Edison, four years after he demonstrated the operation of the incandescent light bulb.[4,5]

Edison's incandescent light bulb employed a conducting filament initially constructed of carbonized bamboo. These filaments lasted only for a few hours before depositing carbon black on the inner glass surface of the bulbs, rendering the bulbs useless. To understand why carbon was being deposited, Edison determined that the carbon was charged as it was evaporated from the filament, and hence the charged carbon constituted a current. Edison placed an additional electrode within an evacuated glass envelope (the other two electrodes comprising the filament electrodes) to measure the flow of charge from the filament. He measured a current only when the added electrode was at a positive electric potential, which indicated the negative charge nature of the charge carriers. Edison was unable to adequately explain his finding, and it went undeveloped. He did file a patent (15 November 1883) on this specialized light bulb because he had anticipated its commercial applications as a voltage regulator. In essence, Edison had discovered the thermionic diode, and this effect was later termed the "Edison effect" by William Preece, a British engineer, in 1885. For this reason Edison is often times called the "father of electronics." Although Edison did nothing further with the Edison effect, it did not go unnoticed by Ambrose Fleming, who, in 1896, noted the rectifying character of the thermionic diode and recognized the electronic implications of electrical rectification.[5] Fleming went on to join the Marconi Wireless Telegraph Co. in England, where in 1904 he developed and patented (under British law) the vacuum tube diode detector for radiofrequency.[5]

Most vacuum tube technology makes use of the property that when a solid is heated to sufficiently high temperatures, some of the electrons possess enough kinetic energy to leave the surface. This phenomenon is known as thermionic emission.[6–8] Richardson employed the Clausius–Clapeyron equation and concluded that the current density J of a hot cathode is given by $J = AT^2 e^{-(W_0/k_B T)}$, which is usually known as the Richardson–Dushman equation, where T is the absolute temperature, W_o is the work function of the metal, k_B is Boltzmann's constant, and A is the Richardson constant, which is $\approx 1.2 \times 10^{+6}$ A/m^2 K^2.[9] This expression was further developed using quantum mechanics by Dushman in 1923 who found that $A = 4\pi m_e k_B^2 e/h^3$, where h is Planck's constant and m_e and e are the mass and the charge of the electron, respectively.[10]

Several articles have used the Richardson–Dushman equation and the Child–Langmuir equation (*vide infra*) to determine either fundamental constants or the work-function of the metal cathode.[11–14] This article is not intended to further this work but will discuss a method for measuring the charge-to-mass ratio of the electron. The unique aspect of this article is that we will use standard vacuum tube diodes rather than diodes designed and constructed specifically for pedagogical use. The vacuum tube diode initially had the role of radiofrequency detection for the transmission of intelligence, where the detection process was accomplished via rectification of the modulated radiofrequency.

The vacuum tube also can be used as a device to generate radio and microwave frequencies, with the latter playing a significant role in the development of radar during World War II. The generation of radio and microwave frequencies can be effected either by setting up oscillations via positive feedback or by vacuum tube oscillators that do not require feedback.[15] The latter methodology was developed by Hull, who pioneered the magnetron.[16] The dynamics of the electrons released via thermionic emission under the influence of orthogonal electric and magnetic fields may be explored using standard vacuum tube pentodes with concentrically related elements. It will be shown in the following that by

using these tubes under special conditions, the electron charge-to-mass ratio may be extracted using techniques similar to those explored by Hull in his development of the split-anode magnetron.

In this paper the use of vacuum tubes to measure the ratio of the charge-to-mass for the electron is highlighted. These experiments provide an alternative to the more traditional ways found in most modern physics laboratories. They provide students with insights to the rich history of vacuum tube technology in addition to introducing them to the early literature on the physics of thermionic emission.

II. THEORY

The concept of a negative space charge surrounding the emitter (cathode) was initially described by Thomson in 1903 (Ref. 5) and systematically analyzed theoretically and experimentally by Child for a parallel plate arrangement of electrodes in 1911 and by Langmuir, who worked out the *I-V* relation for cylindrical electrode geometry in 1913.[17–20] It was shown by Child and Langmuir that the current density for a thermionic diode (regardless of cathode-anode geometry) is proportional to $V^{3/2}$, where V is the anode-cathode electrical potential. For a concentric cylindrical geometry where the cathode (emitter) radius is much smaller than the anode radius, the space charge limited current density is given by

$$ j = \frac{8\pi\varepsilon_0}{9}\left(\frac{2e}{m_e}\right)^{1/2}\frac{V^{3/2}}{r_a}, \tag{1} $$

where j is the line current density, i.e., the current per active length of cathode, r_a is the anode radius, and ε_0 is the permittivity of free space. Equation (1) may be corrected for finite cathode and anode radii, r_c and r_a, respectively, as

$$ j = \frac{8\pi\varepsilon_0}{9}\left(\frac{2e}{m_e}\right)^{1/2}\frac{V^{3/2}}{r_a}\frac{1}{\beta^2}, \tag{2} $$

where

$$ \beta = \alpha - \frac{2}{5}\alpha^2 + \frac{11}{120}\alpha^3 - \frac{47}{3300}\alpha^4 + \dots \tag{3} $$

and $\alpha = \ln(r_a/r_c)$. Equation (2) is the Child–Langmuir equation for cylindrical electrodes. Because $I = jL$, where L is the relevant cathode length, determining the current-voltage characteristic of a thermionic diode yields the charge-to-mass ratio of the electron if we know the relevant geometric parameters of the vacuum tube. Thus,

$$ I = \frac{8\pi\varepsilon_0}{9}\left(\frac{2e}{m_e}\right)^{1/2}\frac{V^{3/2}}{r_a}\frac{1}{\beta^2}L. \tag{4} $$

Recent studies have led to further refinements of the Child–Langmuir law, including extensions to the quantum regime.[21–28]

Tubes in which the trajectories of the electrons are determined by magnetic and electric fields between the cathode and the anode are called magnetrons.[15] If the geometry of the cathode and anode is cylindrically concentric, the structure is called a cylindrical magnetron. The motion of electrons in cylindrical magnetrons in the presence of orthogonal electric and magnetic fields was studied by Hull[16] for various concentric electrode configurations with internal cathodes. Hull[16] assumed that the internal cathode is small and concen-

Fig. 1. Representative vacuum tubes used in this study. The 1V2, 2AV2, and the 1B3-GT are vacuum diodes and were used to measure e/m using the Childs–Langmuir equation (4). The type 41 and type 42 vacuum tubes are power amplifier pentodes. All tube types possess concentric cylindrical geometry.

tric with the cylindrical anode and the magnetic field strength is oriented along the axis of the cathode, and showed that the electric potential of the anode relative to the cathode is given by

$$ V_r = B^2\frac{e}{8m_e}r_m^2\left(1 - \frac{r_c^2}{r_m^2}\right)^2 + \left(\frac{Br_ov_o}{2} - \frac{v_o^2}{2e/m_e}\right)\left(1 - \frac{r_c^2}{r_m^2}\right) - \frac{u_o^2}{2e/m_e}, \tag{5} $$

where $v_o = r_c(d\theta/dt)_c$ and $u_o = (dr/dt)_c$ are the components of the electron's initial velocity at the cathode along the $\hat{\theta}$ and $\hat{r}$ directions, respectively. V_r and B are the electric potential at point r and magnetic field strength, respectively, and r_m is the maximum distance from the central axis that the electron can reach. For $r_m = r_a$ and for a large cylindrical anode radius being large compared to the cathode radius, Eq. (5) becomes

$$ V = B_{\text{crit}}^2\frac{e}{8m_e}r_a^2 + B_{\text{crit}}^2\frac{r_c v_o}{2} - \frac{u_o^2 + v_o^2}{2e/m_e}, \tag{6} $$

where V is the anode (plate) voltage, B_{crit} is equal to the critical magnetic field strength that establishes circular electron trajectories of radius r_a. Because the second and third terms are negligible for reasonable voltages, Eq. (6) reduces to

$$ B_{\text{crit}} = \sqrt{\frac{8m_e}{e}}\frac{V^{1/2}}{r_a}, \tag{7} $$

where V is the potential difference between the filament (cathode) and the cylindrical anode of radius r_a and B_{crit} is the magnetic field strength just sufficient to prevent electrons from reaching the anode. At this field strength, the anode current precipitously drops to zero, and from Eq. (7) we can solve for the charge-to-mass ratio of the electron,

$$ \frac{e}{m_e} = \frac{8V}{B_{\text{crit}}^2}. \tag{8} $$

III. RESULTS AND DISCUSSION

Figure 1 shows a representative sampling of the vacuum tubes used in this experiment. These tubes are easily purchased and range in price from $4.00 to $20.00 and are more readily available than some of the specially designed tubes
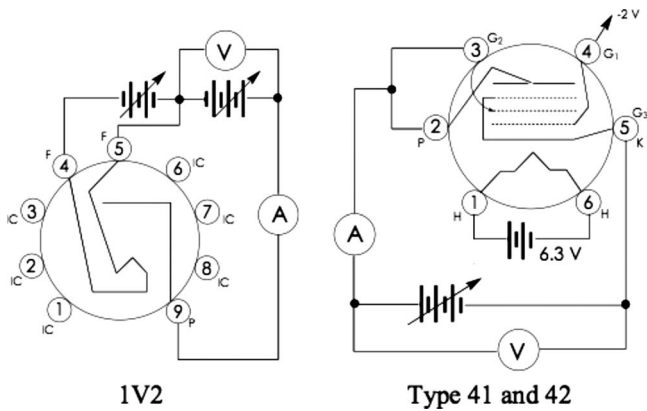
Fig. 2. Representative circuit diagrams used in this study. The 1V2 vacuum diode circuit was used to measure the e/m_e ratio of the electron using Eq. (4). The circuits for other vacuum diodes are similarly constructed. The types 41 and 42 vacuum tube pentodes were used to measure e/m_e using Eq. (8). The tubes were placed in homogeneous magnetic fields (established in a solenoid). All voltages noted in circuit diagrams are approximate and may be adjusted slightly within the manufacturer's suggested range.

Fig. 4. Plot of the plate current as a function of plate voltage for the 2AV2 vacuum tube diode (filament voltage of 1.8 V and filament current of 0.225 A). The data are fit to Eq. (4). The inset shows a plot of the log plate current as a function of the log plate voltage, and the data are fit to the best straight line.

that were previously manufactured for studying thermionic emission.[29] The RCA Receiving Tube Manuals available in many libraries and on the internet are valuable sources of technical information, including pin diagrams, which are important for setting up tube circuits and parameters for establishing working conditions.[30] Reference 31 gives a delightful and complete description of the underlying physics of thermionic emission and basic vacuum tube electronics and is an excellent source for acquainting the novice with the jargon of vacuum tube circuitry. Figure 2 shows schematic diagrams of the tube circuits used in this study.

Figures 3–5 show representative plots of the *I-V* relations for the vacuum diodes 1V2, 2AV2, and 1B3-GT, respectively. All diodes exhibit behavior at low plate voltages that are well fit by the Child–Langmuir equation. Figure 3 also shows *I-V* data at higher voltages where the plate current
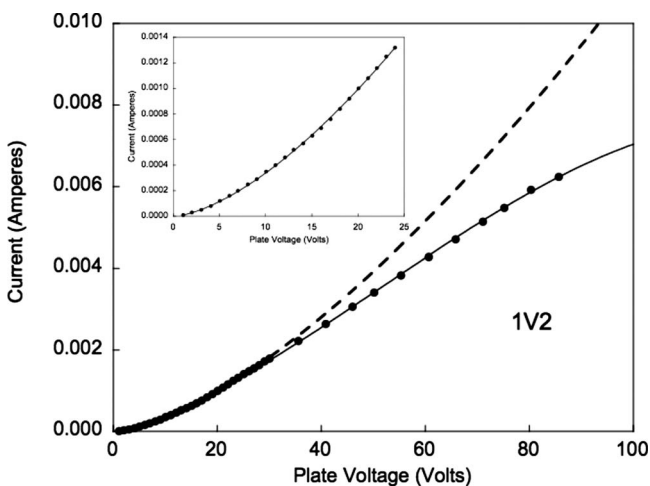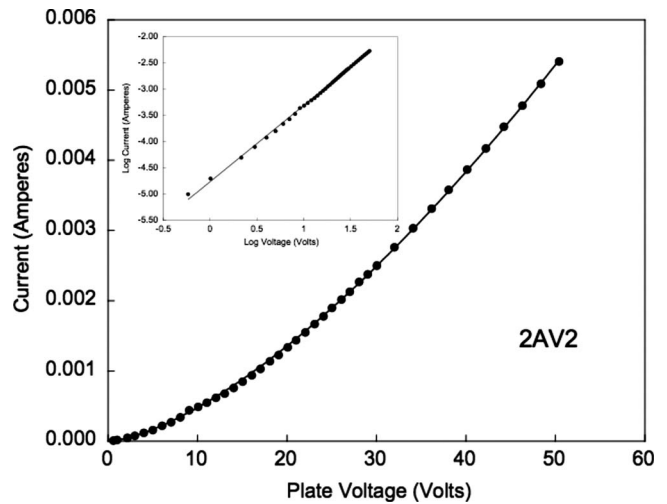
evolves from a space charge limited regime to one that is emission (temperature) limited, a phenomenon known as plate voltage saturation.[29] The inset of Fig. 3 shows the *I-V* relation for the 1V2 diode over a range of plate voltages that is described by the Child–Langmuir expression in Eq. (4). Figures 4 and 5 insets show fits to log *I* as a function of log *V* and are in agreement with Eq. (4). Following the data collection, the tubes were sacrificed to obtain the relevant tube dimensions, such as the cathode and anode radii along with the active length of the cathode filament. These data and the calculated electron charge-to-mass ratios are given in Table I. The calculation of e/m_e was corrected for the finite cathode radius using the data tabulated by Langmuir and Blodgett[20] and plotted in Fig. 6. The charge-to-mass ratios determined by this method give errors of $\leq 10\%$ (see Table I), which are comparable to the errors typically found using the Bainbridge method.[3] However, this method gives stu-

Fig. 3. Plot of the plate current as a function of plate voltage for the 1V2 vacuum tube diode (filament voltage of 0.63 V and filament current of 0.3 A). The data are fit to a $V^{3/2}$ relation (dashed line). The curve is a best fit to the data and is only to guide the eye. The inset shows a plot of the plate current as a function of plate voltage in the region where the Child–Langmuir relation is satisfied. The data for this plot are fit to Eq. (4) (solid line).
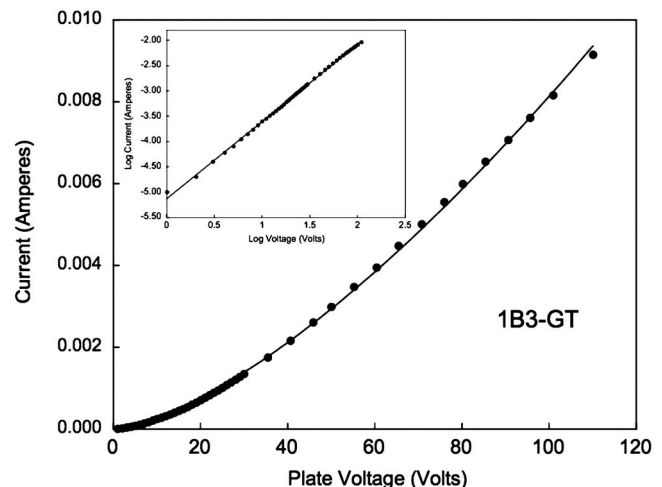

Fig. 5. Plot of the plate current as a function of plate voltage for the 1B3-GT vacuum tube diode (filament voltage of 1.25 V and filament current of 0.2 A). The data are fit to Eq. (4). The inset shows a plot of log plate current as a function of log plate voltage, and the data are fit to the best straight line.

Table I. Vacuum tube diode physical parameters and determination of the electron charge-to-mass ratio. The tube type is the manufacturer's tube designation.

	Tube Type		
	1V2	2AV2	1B3GT
Cathode radius (cm)	0.0318	0.0533	0.0241
Anode radius (cm)	0.592	0.591	0.720
Effective length (cm)	0.534	0.638	0.602
r_a/r_c	18.64	11.09	29.88
Langmuir β	1.081	1.010	1.091
e/m_e (C/kg)	$1.691 \times 10^{+11}$	$1.681 \times 10^{+11}$	$1.944 \times 10^{+11}$
% error	3.70	4.27	10.7

dents hands-on experience with the use of meters, power supplies, wrapping solenoids, and with interfacing the experimental setup using LABVIEW or similar interface software.

The value of e/m_e was also determined using the cylindrical magnetron method. Figure 7 shows the plate current as a function of magnetic field for type 41 and type 42 pentodes that have been configured as magnetrons. In this experiment the tube is placed inside a solenoid (100 turns/m) such that the direction of the magnetic field is perpendicular to the radially directed electric field between the coaxial cathode and anode. The magnetic field strength within the solenoid was calculated using $B=\mu_o n i$, where μ_o is the permeability of free space and n is the linear loop density, and i is the current. The potential difference in Eq. (7) is the cathode (filament)-anode (plate) voltage. The control grid voltage was set to -2.0 V (nominally), and the plate and screen grid voltages were set to the same value (given in Fig. 7 and in Table II), with the suppressor grid connected to the cathode. The control grid and screen grid electric potentials do not affect the result because they are independent of the electric potential distribution. The intersection of the straight lines established from the low magnetic field horizontal portion of the plot and the steeply decreasing section of the sigmoid-plot was taken to define the critical field B_{crit} of the current-field characteristic (see Fig. 7). The critical field strengths at various plate-screen voltages along with the determined
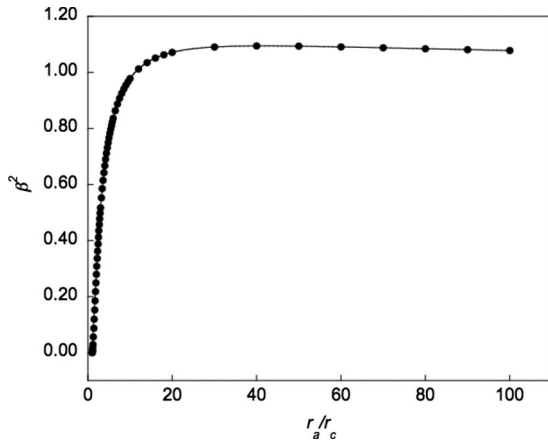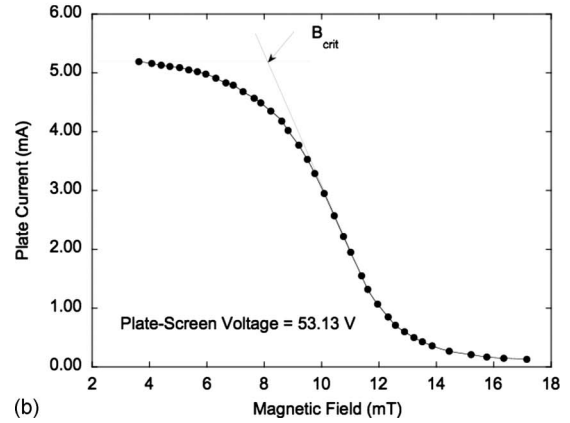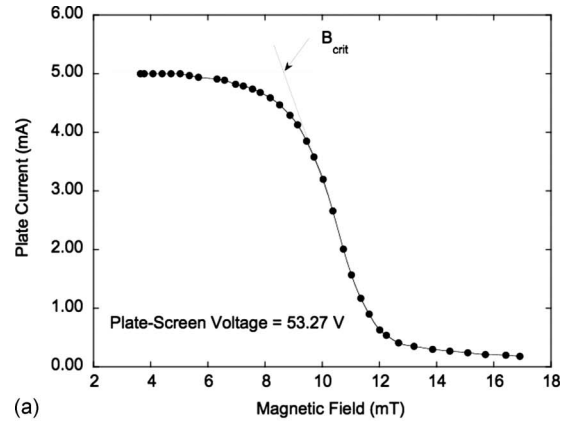

Fig. 7. Plot of the plate current as a function of magnetic field for (a) type 41 and (b) type 42 pentodes. The data at magnetic field strengths below and above the cutoff were fit to best straight lines, and the intersection of these lines was used to determine the cutoff magnetic field strength B_{crit}. In both plots the grid voltage was set to -2.0 V and the plate and screen grid voltages were set to the values shown in each plot. The smooth line through the data is to guide the eye only and is not meant a fit to theory.

charge-to-mass ratios are tabulated in Table II for types 41 and 42 pentodes. As with the vacuum tube diode method based on Eq. (4), the errors obtained using the magnetron method are ≤10%.

Theoretically, the anode current versus magnetic field plot should exhibit a step function behavior with the anode current going to zero at the critical magnetic field. The sigmoi-

Fig. 6. Plot of β^2 as a function of the ratio of the radius of the anode to the radius of the cathode for a concentric cylindrical geometry (r_a/r_c). Data taken from Ref. 20.

Table II. Electron charge-to-mass ratio from the critical magnetic field strength B_{crit} in the type 41 and type 42 vacuum pentodes.

	Type 41		
Plate-screen voltage (V)	32.07	53.27	106.02
Experimental B_{crit} (mT)	6.79	8.63	11.48
Theoretical B_{crit} (mT)	6.37	8.21	11.58
e/m_e (C/kg)	1.55×10^{-11}	1.62×10^{-11}	1.79×10^{-11}
% error	11.99	9.50	1.79
	Type 42		
Plate-screen voltage (V)	32.05	53.13	106.02
Experimental B_{crit} (mT)	6.23	8.13	10.52
Theoretical B_{crit} (mT)	6.37	8.20	11.58
e/m_e (C/kg)	1.84×10^{-11}	1.79×10^{-11}	2.13×10^{-11}
% error	4.48	1.71	21.2

dal character may be due to misalignment of the tube within the solenoid, anode edge effects, alteration of the electric potential due to space charge effects, electron-electron collisions resulting in one electron gaining energy at the expense of the other, and the distribution of initial electron velocities at the cathode.

IV. SUMMARY

The accepted value of the charge-to-mass ratio e/m_e of the electron is $1.758\,820\,150(44) \times 10^{-11}$ C/kg. By using the standard Bainbridge tube technique, we can obtain results with percent errors of $<10\%$ of this value.[3] In this paper, two methods have been described and studied using thermionic emission of metals as the fundamental phenomenon. These methods afford opportunities for the determination of the e/m_e ratio with comparable percentage errors without using the Bainbridge tube method. Moreover, some of the current apparatuses do not require students to have much hands-on laboratory experience, and the student is exposed to phenomena and technological historical developments that are typically not deeply covered in current physics curricula.

[1] K. T. Bainbridge, "The specific charge of the electron," Am. J. Phys. **6**, 35–36 (1938).

[2] J. E. Price, "Electron trajectory in an e/m experiment," Am. J. Phys. **55**, 18–22 (1987) and references therein.

[3] W. J. Thompson, "Determining e/m with a Bainbridge tube: Less data, more physics," Am. J. Phys. **58**, 1019–1020 (1990).

[4] J. B. Johnson, "Contribution of Thomas A. Edison to thermionics," Am. J. Phys. **28**, 763–773 (1960).

[5] P. A. Redhead, "The birth of electronics: Thermionic emission," J. Vac. Sci. Technol. A **16**, 1394–1401 (1998) and references therein.

[6] S. Dushman, "Thermionic emission," Rev. Mod. Phys. **2**, 381–476 (1930).

[7] I. Langmuir and K. T. Compton, "Electrical discharges in gases. Part II. Fundamental phenomena in electrical discharges," Rev. Mod. Phys. **3**, 191–257 (1931).

[8] C. Herring and M. H. Nichols, "Thermionic emission," Rev. Mod. Phys. **21**, 185–270 (1949).

[9] O. W. Richardson, *Emission of Electricity from Hot Bodies* (Longmans, Green, and Co., London, 1916), and references therein.

[10] S. Dushman, "Electron emission from metals as a function of temperature," Phys. Rev. **21**, 623–636 (1923).

[11] S. B. Brody and S. R. Singer, "Experiment on thermionic emission," Am. J. Phys. **38**, 1044 (1970).

[12] J. G. Todd, "An experiment on electron emission," Am. J. Phys. **39**, 1159–1163 (1971).

[13] T. B. Greenslade, "A new tube for Richardson–Dushman experiments," Am. J. Phys. **59**, 957–958 (1991).

[14] R. J. Umstattd, C. G. Carr, C. L. Frenzen, J. W. Lugisland, and Y. Y. Lau, "A simple physical derivation of Child–Langmuir space limited emission using vacuum capacitance," Am. J. Phys. **73**, 160–163 (2005).

[15] P. Parker, *Electronics* (Edward Arnold and Co., London, 1950).

[16] A. W. Hull, "The effect of a uniform magnetic field on the motion of electrons between coaxial cylinders," Phys. Rev. **18**, 31–57 (1921).

[17] C. D. Child, "Discharge from hot CaO," Phys. Rev. **32**, 492–511 (1911).

[18] I. Langmuir, "The effect of space charge and residual gases on thermionic currents in high vacuum," Phys. Rev. **2**, 450–486 (1913).

[19] I. Langmuir, "The effect of space charge and initial velocities on the potential distribution and thermionic current between parallel plane electrodes," Phys. Rev. **21**, 419–435 (1923).

[20] I. Langmuir and K. B. Blodgett, "Currents limited by space charge between coaxial cylinders," Phys. Rev. **22**, 347–356 (1923).

[21] Y. Y. Lau, D. Chernin, D. G. Colombant, and P.-T. Ho, "Quantum extension of Child–Langmuir law," Phys. Rev. Lett. **66**, 1446–1449 (1991).

[22] J. W. Luginsland, Y. Y. Lau, and R. M. Gilgenbach, "Two-dimensional Child–Langmuir law," Phys. Rev. Lett. **77**, 4668–4670 (1996).

[23] Y. Y. Lau, "Simple theory for the two-dimensional Child–Langmuir law," Phys. Rev. Lett. **87**, 278301-1–3 (2001).

[24] J. W. Lugisland, Y. Y. Lau, R. J. Umstattd, and J. J. Watrous, "Beyond the Child–Langmuir law: A review of recent results on multidimensional space-charge limited flow," Phys. Plasmas **9**, 2371–2376 (2002).

[25] L. K. Ang, T. J. T. Kwan, and Y. Y. Lau, "New scaling of Child–Langmuir law in the quantum regime," Phys. Rev. Lett. **91**, 208303-1–4 (2003).

[26] R. R. Puri, D. Biswas, and R. Kumar, "Generalization of the Child–Langmuir law for nonzero injection velocities in a planar diode," Phys. Plasmas **11**, 1178–1186 (2004).

[27] O. Sutherland, A. Ankiewicz, and R. Boswell, "Generalization of the Langmuir–Blodgett laws for a nonzero potential gradient," Phys. Plasmas **12**, 033103-1–7 (2005).

[28] A. V. Soldatov, "Space-charge-limited current in a plane vacuum diode discharged by an electron current pulse," Plasma Phys. Rep. **31**, 300–305 (2005).

[29] There are numerous sources on the Web for acquiring tubes. Some favorites are ⟨www.vacuumtubesinc.com⟩, ⟨www.vacuumtubes.net⟩, ⟨www.thetubestore.com⟩, and ⟨www.vacuumtube.com⟩.

[30] *RCA Receiving Tube Manual, RC-30 (Technical Series RC-30)* (Radio Corporation of America, Harrison, NJ, 1973).

[31] J. F. Rider, *Inside the Vacuum Tube* (John F. Rider, New York, 1945).